



Contents lists available at ScienceDirect

Spectrochimica Acta Part A: Molecular and Biomolecular Spectroscopy

journal homepage: www.elsevier.com/locate/saa

Synthesis, growth, structure and spectroscopic characterization of a new organic nonlinear optical hydrogen bonding complex crystal: 3-Carboxyl anilinium p-toluene sulfonate



E. Selvakumar^a, G. Anandha babu^b, P. Ramasamy^b, Rajnikant^c, T. Uma Devi^d, R. Meenakshi^e, A. Chandramohan^{a,*}

^a Department of Chemistry, SRMV College of Arts and Science, Coimbatore 641020, TN, India

^b Centre for Crystal Growth, SSN College of Engineering, Kalavakkam 603110, TN, India

^c X-ray Crystallography Laboratory, Post-Graduate Department of Physics, University of Jammu, Jammu Tawi 180006, India

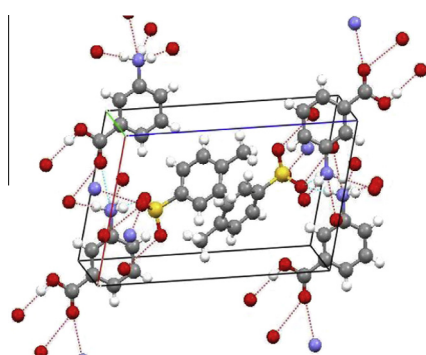
^d Department of Physics, Government Arts College for Women (Autonomous), Pudukottai 622001, TN, India

^e Department of Physics, Cauvery College For Women, Trichy 600018, TN, India

HIGHLIGHTS

- Good organic NLO crystal grown by solution growth technique.
- The title crystal has wide optical transparency window between 300 nm and 2500 nm.
- The title complex crystal thermally stable up to 255 °C.
- Structural, optical and thermal properties were discussed.

GRAPHICAL ABSTRACT



ARTICLE INFO

Article history:

Received 5 September 2013

Received in revised form 5 January 2014

Accepted 10 January 2014

Available online 30 January 2014

Keywords:

Crystal growth

X-ray diffraction

Hydrogen bonding complex

Nonlinear optical material

ABSTRACT

A new organic nonlinear optical hydrogen bonding complex salt of 3-carboxyl anilinium p-toluene sulfonate has been synthesized and highly transparent good quality single crystals of it were successfully grown employing slow solvent evaporation solution growth technique at ambient temperature. The ¹H and ¹³C NMR spectra were recorded to establish the molecular structure. The single crystal XRD analysis carried out reveals that the title salt crystallizes in monoclinic crystal system with non-centrosymmetric P2₁ space group. The FT-IR spectrum was recorded to confirm the presence of various functional groups in the grown title crystal. The UV-Vis-NIR transmission spectrum was recorded to apprehend the suitability of the single crystal of the title salt for various optical and NLO applications. The TG/DTA thermal analysis was performed to establish the thermal stability of the crystal. The SHG activity in the grown crystal was identified employing the modified Kurtz–Perry powder test. The electronic charge distribution and reactivity of the molecules within the title complex was studied by HOMO and LUMO analysis and the molecular electrostatic potential (MEP) of the title crystal was performed using the B3LYP method.

© 2014 Elsevier B.V. All rights reserved.

Introduction

There is an ever-growing demand for organic NLO crystals with very high SHG activity owing to their potential applications in

* Corresponding author. Tel.: +91 9994283655.

E-mail address: dracmsrmvcas@gmail.com (A. Chandramohan).

frequency conversion, frequency mixing, optical data storage and electro optic modulation, etc. [1–8]. Organic nonlinear optical materials have gained considerable attention than the inorganic materials, as they have high optical nonlinearity and synthetic flexibility [9]. Organic materials allow one to fine tune their optical properties through molecular engineering and chemical synthesis [10]. More than 70% of organic compounds crystallize in centrosymmetric space groups due to the predominant anti-parallel π -stacking between the aromatic rings as a consequence of dipolar interactions [11,12]. As a result, they are unable to exhibit the SHG activity. To overcome this major problem, various molecular engineering approaches have been suggested to form acentric crystal structures. Out of the various strategies, the hydrogen bonding interactions play a pivotal role in creating acentric crystal structure in organic molecules by orienting the molecular dipoles in a head-to-tail manner and also enhance the mechanical and thermal stabilities [13–17]. Hydrogen bonding supplemented by a mutual polarization will also give rise to an efficient second harmonic generation [18]. Simple donor-acceptor *o*-, *p*- and *m*-disubstituted benzene derivatives represent a peculiar type of molecules possessing nonlinear optical properties both in their solutions and in solid states [19]. This is due to the interaction between the donor and acceptor group via aromatic ring induces an asymmetric electronic distribution, leading to an enhanced nonlinear optical response [20,21]. 3-amino benzoic acid contains an electron withdrawing $-\text{COOH}$ group and electron releasing $-\text{NH}_2$ group connected through π -conjugated system of the aromatic ring [22,23]. *p*-toluene sulfonic acid is a strong acid forms strong hydrogen bonding complexes with bases like amines. The *m*-disubstituted benzene derivatives appear to have the tendency to crystallize in non-centrosymmetric space groups relative to their ortho and para analogues [24]. Based on the above said aspects, in the present investigation we present the synthesis, growth and spectroscopic characterization of SHG active organic hydrogen bonding complex salt 3-carboxyl anilinium *p*-toluene sulfonate (CATS). The title material was synthesized and the single crystals were grown and characterized through electronic, vibrational absorptions, nuclear magnetic resonance spectral studies, and TG-DTA and Nonlinear optical studies. On the basis of the above studies, the molecular structure, optical property, proton transfer interaction and thermal stability of the title complex have been reported.

Experimental procedure

Material synthesis

AR grade 3-amino benzoic acid and *p*-toluene sulfonic acid were purchased and used as such without further purification. Equimolar solutions of 3-amino benzoic acid and *p*-toluene sulfonic acid were prepared separately in ethanol and Millipore water respectively and henceforth mixed together. The resulting solution was stirred well for about an hour using a temperature controlled magnetic stirrer at room temperature. The obtained product was filtered off, dried and repeatedly recrystallized in ethanol to improve the purity of the synthesized compound. The reaction involved is represented in Fig. S1.

Solubility and crystal growth

A saturated ethanolic solution of CATS was prepared, stirred well for about an hour and heated slightly to ensure the complete dissolution of the material. The solution was then filtered through a Whatman 41 grade filter paper to remove the suspended impurities completely. The clear filtrate was kept aside unperturbed in an atmosphere conducive for the growth of single crystals. Well grown good optical quality single crystals were harvested in about

fifteen days time. The photograph of the as-grown crystals is depicted in Fig. S2.

Characterization

To confirm the molecular structure of CATS crystal, the ^1H and ^{13}C NMR spectra were recorded employing a Bruker 500 MHz spectrometer in deuterated solvents using TMS as the internal reference standard. The crystal structure was determined from the single-crystal X-ray diffraction data obtained with an X'calibur CCD area-detector diffractometer (Graphite – monochromated, $\text{Mo K}\alpha_1 = 0.713$). The data were collected at 25 °C and the structure was solved by direct methods using the program SHELXS-97 [25] and refined by full-matrix least-squares method using SHELXL-97 [26]. The H-atoms could all be located in Fourier difference maps. FT-IR spectrum was recorded using potassium bromide pellet method employing a Perkin Elmer FT-IR spectrometer in the range 4000–450 cm^{-1} . The UV-Vis-NIR transmittance spectrum of CATS was recorded employing a VARIAN CARY 5E UV-Vis-NIR spectrophotometer. The TGA and DTA studies were carried out on a PERKIN ELMER DIAMOND instrument with a heating rate of 10 °C/min in the temperature range from 20 to 400 °C in nitrogen atmosphere. Quantitative estimation of relative SHG efficiency of CATS crystal with respect to KDP was made by the modified Kurtz and Perry powder technique. The electronic property and charge transfer interaction of the title complex was studied by B3LYP method.

Results and discussion

NMR spectral studies

The ^1H NMR spectrum of CATS crystal is shown in Fig. S3. The intense singlet signal appearing at δ 2.36 ppm is due to the three methyl protons of *p*-toluene sulfonate moiety in the salt. The C3 and C5 aromatic protons of the same kind in the same moiety exhibit a doublet centered at δ 7.21 ppm. The complex multiplet appearing from δ 7.63 to 7.65 ppm is attributed to the C4 and C6 aromatic protons in the same chemical environment in 3-carboxyl anilinium moiety. The doublet centered at δ 7.70 ppm owes to the C2 and C6 aromatic protons of the same kind in *p*-toluene sulfonate moiety in the salt. The C2 aromatic proton of 3-carboxyl anilinium moiety stands responsible for the singlet signal at δ 8.06 ppm. The multiplet signal appearing from δ 8.10 ppm to δ 8.13 ppm has been assigned to C5 aromatic proton of the same moiety. Thus appearance of six distinct proton signals confirms the molecular structure of the salt crystal.

The ^{13}C NMR spectrum of CATS crystal is depicted in Fig. S4. The appearance of 12 distinct carbon signals in the spectrum establishes the molecular structure of the title salt. The carbon signal appearing in the downfield at δ 166 ppm is attributed to the highly deshielded carboxyl carbon of the 3-carboxyl anilinium moiety in the salt. The carbon signal due to the methyl carbon is exhibited at δ 19.953 ppm in the upfield. The aromatic carbon atoms of 3-carboxyl anilinium and *p*-toluene sulfonate moieties appear in the range from δ 123.95 to 141.86 ppm and their respective assignments are given in Table 1.

Single crystal X-ray diffraction analysis

Single crystals suitable for X-ray crystallographic analysis were selected following an examination under a polarizing microscope. X-ray intensity data of 2912, reflections (of which 2627 were unique) were collected on a X'calibur CCD area-detector diffractometer equipped with graphite monochromated $\text{Mo K}\alpha$ radiation ($\lambda = 0.71073$ Å). The cell dimensions were determined by least-

Table 1
¹³C NMR spectral data of CATS.

δ Value (ppm)	Assignment
166.511	Carboxyl carbon of 3-carboxyl anilinium moiety
141.868	C1 Carbon of p-toluene sulfonate moiety
140.466	C1 Carbon of 3-carboxyl anilinium moiety
132.785	C3 Carbon of 3-carboxyl anilinium moiety
131.070	C2 & C6 carbon atoms of same kind in p-toluene sulfonate moiety
130.136	C2 Carbon of 3-carboxyl anilinium moiety
129.763	C4 Carbon of 3-carboxyl anilinium moiety
128.499	C6 Carbon of 3-carboxyl anilinium moiety
127.204	C5 Carbon of 3-carboxyl anilinium moiety
125.514	C3 & C5 carbon atoms of same kind in p-toluene sulfonate moiety
123.952	C4 carbon p-toluene sulfonate moiety
19.953	Methyl carbon of p-toluene sulfonate moiety

squares fit of angular settings of 2912 reflections in the θ range 3.41–28.93°. The intensities were measured by ω scan mode for 2θ ranges from 3.62° to 24.99°. The data were corrected for Lorentz polarization and absorption factors. The structure was solved by direct methods using SHELXS97. All non-hydrogen atoms of the molecule were located in the best E-map. Full-matrix least-squares refinement was carried out using SHELXL97 and the final refinement cycles converged to an $R = 0.0420$ and $wR (F2) = 0.1127$ for the observed data. Residual electron densities ranged from 0.332 to 0.187 Å³. The geometry of the molecule was calculated using the WinGX [27] and PARST [28] softwares. The crystal data and details of the data collection and the structure refinement are given in Table 2. The selected bond lengths and bond angles of CATS are given in Table 3. The hydrogen bonding dimensions are given in Table 4. Fig. 1 shows the ORTEP view of the molecule drawn at 40% probability thermal displacement ellipsoids with the atom numbering scheme. The packing arrangement of molecule viewed down the b -axis is shown in Fig. 2.

FT-IR spectral studies

The recorded FT-IR spectrum is shown in Fig. 3. The assignment of the well defined bands in the infrared spectrum is given in Table 5. The O–H asymmetric stretching vibration of carboxylic group is observed at 3437 cm⁻¹. The N⁺–H stretching vibration

Table 2
 Crystal data and structure refinement of CATS.

Empirical formula	C14 H15 N O5 S
Formula weight	309.33
Crystal system, space group	Monoclinic, P2 ₁
Unit cell dimensions	$a = 8.4228(3) \text{ \AA}$ $b = 6.6068(2) \text{ \AA}$ $c = 13.6637(5) \text{ \AA}$
Volume	741.69(4) Å ³
Z	2
Temperature	293(2) K
Reflections used	7802
Theta range for data collection	3.4348, 29.0403
Density	1.385 Mg/m ³
F(000)	324
Absorption coefficient	0.238
Radiation wavelength	0.71073 Å
Radiation type	MoK α_1
Reflections collected/unique	2912, 2627
Number restraints	1
R factor all	0.0432
R factor gt	0.0373
wR factor ref	0.0947
wR factor gt	0.0900
Goodness fit	1.061
Theta max	0.997
Final residual electron density	-0.289 > ρ > 0.044 Å ⁻³

Table 3
 Selected bond lengths and bond angles of CATS.

Bond	Length (Å)	Bond	Angles (°)
S1–O1	1.4414(17)	O1–S1–O2	114.00(15)
O9–C8	1.203(2)	O2–S1–C11	105.68(11)
O10–C8	1.315(2)	O3–S1–C11	104.71(11)
C1–C6	1.378(3)	C6–C1–C2	122.02(16)
C1–N7	1.461(2)	C2–C1–N7	118.73(16)
C2–C3	1.389(3)	C1–C2–C3	118.79(18)
C5–C8	1.491(3)	C3–C4–H4	119.9
C6–H6	0.9300	C5–C4–H4	119.9
N7–H71	0.97(4)	C4–C5–C6	120.17(18)
C11–C16	1.362(4)	C1–C6–C5	118.53(16)
C12–C13	1.379(4)	C5–C6–H6	120.7
C12–H12	0.9300	C1–N7–H71	106(2)
C13–C14	1.348(5)	C1–N7–H72	110.6(16)
C14–C15	1.367(5)	C1–N7–H73	109.6(14)
C14–C17	1.519(5)	H71–N7–H73	113(3)
C15–C16	1.377(5)	H72–N7–H73	110(2)

Table 4
 Hydrogen bonding geometry for CATS.

D–H...A	D–H	H...A	D–A	<D–A
O (10)–H(10)...O(1)	0.92(3)	1.88(3)	2.797(2)	175(3)
N (7)–H(71)...O(2)	0.97(4)	1.79(4)	2.753(3)	172(3)
N (7)–H(72)...O(3)	0.86(3)	1.99(3)	2.843(3)	175(2)
N (7)–H(73)...O(3)	0.95(3)	1.97(3)	2.898(3)	165(2)

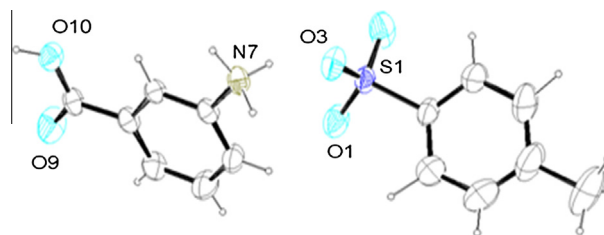


Fig. 1. ORTEP view of CATS crystal.

appears at 3074 cm⁻¹. The aromatic C–H asymmetric stretching vibration appears at 2921 cm⁻¹. The C–H stretching frequency of CH₃ group in the p-toluene sulfonate moiety is observed at 2622 cm⁻¹. The strong absorption band at 1725 cm⁻¹ owes to the C=O stretching vibration of the carboxyl group of 3-carboxyl anilinium moiety. The asymmetric and symmetric bending vibrations of NH₃⁺ group appear respectively at 1603 and 1495 cm⁻¹. The aromatic C=C stretching vibrations produce bands at 1527, 1456 and 1414 cm⁻¹. The O–H in plane bending vibration is observed at 1310 cm⁻¹. The C–N stretching vibration appears as a strong band at 1162 cm⁻¹. The characteristic SO₃⁻ asymmetric and symmetric stretching vibrations of p-toluene sulfonate group appear respectively at 1269 and 1032 cm⁻¹. The aromatic C–H in plane bending vibrations are observed at 1124 and 1008 cm⁻¹. The aromatic C–H out of plane bending vibrations exhibit bands at 816 and 800 cm⁻¹. The frequencies less than 500 cm⁻¹ in the spectrum are due to the skeleton vibrations.

UV–Vis–NIR spectral analysis

The UV–Vis–NIR transmission spectrum of CATS crystal is shown in Fig. 4. It is evident from the spectrum that there is no significant absorption in the entire visible region and NIR region. The lower cutoff wavelength occurs at 300 nm and the crystal exhibits 80% transmittance. This lower cutoff wavelength combined with very good transmittance make the title crystal well suited for the

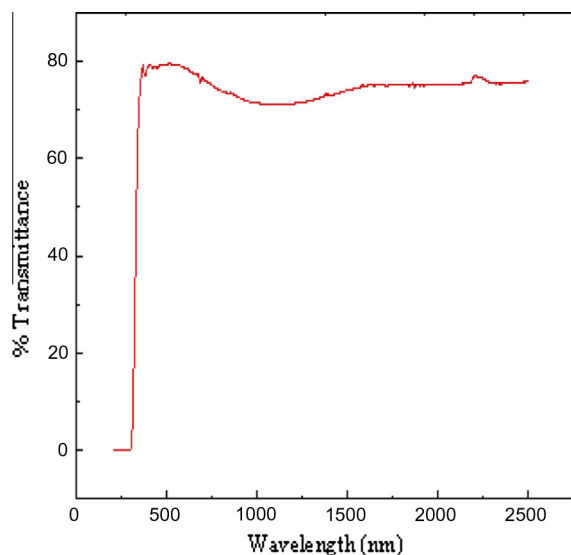


Fig. 4. UV-Vis transmittance spectrum of CATS.

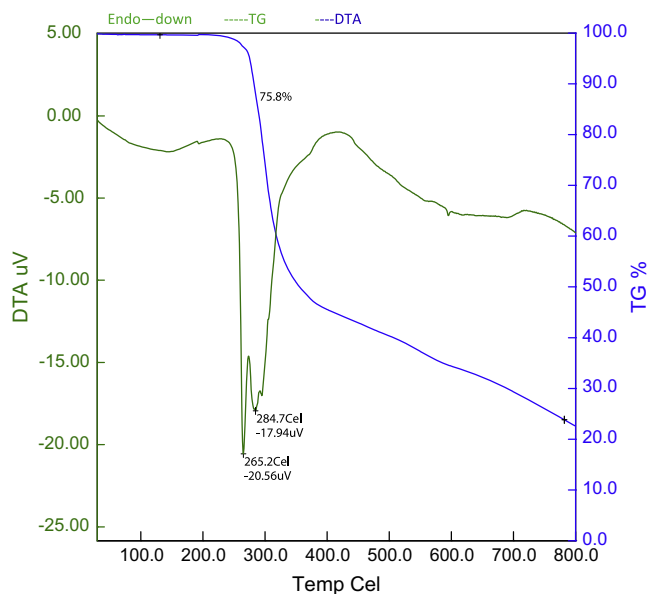
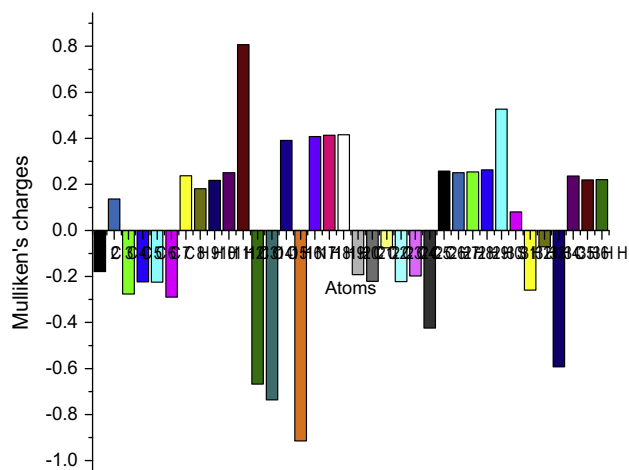


Fig. 5. TG and DTA thermogram of CATS.

indications as red color, the maximum positive region which preferred site for nucleophilic attack symptoms as blue color. The importance of MEP lies in the fact that it simultaneously displays molecular size, shape as well as positive, negative and neutral electrostatic potential regions in terms of color grading and is very useful in research of molecular structure with its physiochemical property relationship [30]. The resulting surface simultaneously displays molecular size and shape and electrostatic potential value. In the present study, a 3D plot of MEP of title crystal is drawn in Fig. S5. The MEP is a plot of electrostatic potential mapped onto the constant electron density surface. The different values of the electrostatic potential at the surface are represented by different colors. Potential increases in the order red < orange < yellow < green < blue. The blue indicates the strongest attraction and red indicates the strongest repulsion. Regions of negative $V(r)$ are usually associated with the lone pair of electronegative atoms. As can be seen from the MEP map of the title crystal, while regions having the negative potential are over the electronegative atom (nitrogen and oxygen atoms), the regions having



was established by TG/DTA studies. The SHG efficiency was shown to be comparable to that of the reference KDP.

Appendix A. Supplementary material

Supplementary data associated with this article can be found, in the online version, at <http://dx.doi.org/10.1016/j.saa.2014.01.035>.

References

- [1] R.W. Munn, C.N. Ironside, *Principles and Applications of Nonlinear Optical Materials*, Chapman & Hall, London, 1993.
- [2] L.R. Dalton, P.A. Sullivan, B.C. Olbricht, D.H. Bale, J. Takayesu, S. Hammond, H. Rommel, B.H. Robinson, *Tutorials in Complex PhotonicMedia*, SPIE, Bellingham, WA, 2007.
- [3] T. Kaino, B. Cai, K. Takayama, *Adv. Funct. Mater.* 12 (2002) 599.
- [4] F. Pan, G. Knopfle, C. Bosshard, S. Follonier, R. Spreiter, M.S. Wong, P. Gunter, *Appl. Phys. Lett.* 69 (1996) 13.
- [5] M. Thakur, J. Xu, A. Bhowmilk, L. Zhou, *Appl. Phys. Lett.* 74 (1999) 635.
- [6] W. Geis, R. Sinta, W. Mowers, S.J. Deneault, M.F. Marchant, K.E. Krohn, S.J. Spector, D.R. Calawa, T.M. Lyszczarz, *Appl. Phys. Lett.* 84 (2004) 3729.
- [7] A. Schneider, M. Neis, M. Stillhart, B. Ruiz, R.U.A. Khan, P. Gunter, *J. Opt. Soc. Am. B* 23 (2006) 1822.
- [8] B. Ferguson, Z.-C. Zhang, *Nat. Mater.* 1 (2002) 26.
- [9] Tanusri pal, Tanusree Kar, Gabriele Bocelli, Lara Rigi, *Cryst. Growth Des.* 3 (2003) 13.
- [10] A. Datta, S.K. Pati, *J. Chem. Phys.* 118 (2003) 8420.
- [11] S.C. Abrahams, J.M. Robertson, *Acta Cryst.* 1 (1948) 252.
- [12] J. Donhue, K.N. Trueblood, *Acta Cryst.* 9 (1956) 960.
- [13] A. Datta, S.K. Pati, *Chem. Soc. Rev.* 35 (2006) 1305.
- [14] A. Datta, S. K. Pati, *Chem. Eur. J.* 11 (2005) 4961.
- [15] A. Datta, D. Davis, K. Sreekumar, S.K. Pati, *J. Phys. Chem. A* 109 (2005) 4112.
- [16] A. Datta, S.K. Pati, *J. Phys. Chem. A* 108 (2004) 320.
- [17] A. Criado, M.J. Dianez, S.P.L. Garrido, I.M. Fernandes, M.E. Belsley, M. de Gomes, *Acta Crystallogr. C* 56 (2000) 888.
- [18] J. Zaccaro, J.P. Salvestrini, A. Ibanez, P. Ney, M.D.J. Fontana, *Opt. Soc. Am.* 17B (2000) 427.
- [19] J.A.R.P. Sarma, J. Laximikanth, K. Banuprakash, *Chem. Mater.* 7 (1995) 1843–1848.
- [20] A. Dulcic, C. Sauteret, *J. Chem. Phys.* 69 (1978) 3453.
- [21] B.F. Levine, *J. Chem. Phys.* 63 (1975) 115.
- [22] B.F. Levine, *Chem. Phys. Lett.* 37 (1976) 516.
- [23] R.N. Raj, K.B.R. Varma, *J. Cryst. Growth* 285 (2005) 111.
- [24] Vincent Crasta, V. Ravindrachary, S. Lakshmi, S.N. Pramod, M.A. Shridar, J. Shashidhara Prasad, *J. Cryst. Growth* 275 (2005) e329.
- [25] G.M. Sheldrick, *SHELX97*, University of Gottingen, Germany, 1997.
- [26] L. Farrugia, *J. Appl. Crystallogr.* 30 (1997) 565.
- [27] L. Farrugia, *J. Appl. Crystallogr.* 32 (1999) 837.
- [28] M. Nardelli, *J. Appl. Crystallogr.* 28 (1995) 659.
- [29] S.K. Kurtz, T.T. Perry, *J. Appl. Phys.* 39 (1968) 3798.
- [30] J.S. Murray, K. Sen, *Molecular Electrostatic Potentials, Concepts and Applications*, Elsevier, Amsterdam, 1996.
- [31] S.M. Soliman, *J. Mol. Struct.* 1048 (2013) 308–320.